UNIVERSITY OF NAPLES FEDERICO II

PH.D. PROGRAM IN

BIOMORPHOLOGICAL AND SURGICAL SCIENCES

XXX Cycle

(Years 2014-2017)

Chairman: Prof. Alberto Cuocolo

PH.D. THESIS

TITLE

MR imaging of tenosynovial giant cell tumor: additional value of a T2*-weighted gradient echo sequence

TUTOR

Prof. Alberto Cuocolo

PH.D. STUDENT

Dr. Marco Catalano

INDEX

Title:

MR imaging of tenosynovial giant cell tumor: additional value of a T2*-weighted gradient echo sequence

Background/Purpose:

To evaluate the role of a T2*-weighted gradient echo (GRE) sequence added to a standard MR imaging protocol in assessing the iron content of tumor tissue and the extent of joint involvement in patients with tenosynovial giant cell tumor (TGCT).

Methods and Materials:

MR studies of 58 patients (mean age: 36,7 years; 35 female, 23 male) with histologically proven TGCT (knee: n=44, hip: n=5, ankle: n=5, elbow: n=1, tarsus: n=1, tendon sheath: n=2) obtained prior to surgical resection were retrospectively analyzed. All examinations were performed according to a standardized protocol which in addition to T1-, T2-weighted and CE SE/TSE sequence a T2*-weighted GRE sequence is included. Standard and GRE images were separately analyzed by three independent observers with regard to 1) relative iron content of tumor tissue as determined by the distribution and extent of blooming (susceptibility) artifacts (0-absent, 1-focal (<30%), 2-moderate/confluent (30-70%), 3-massive/diffuse (>70%)) and 2) the identification of tumor tissue on GRE images in joint compartments which

appeared uninvolved on images of standard sequences. Intraoperative and histologic findings served as the standards of reference. All histologic specimens were reviewed and iron content was graded corresponding to the above mentioned classification by an experienced pathologist.

Results:

59% of the lesions were classified (WHO 2013) as localized and 41% as diffuse TGCTs. On histologic review, the iron content was graded as follows: 0: n=2, 1: n=13, 2: n=29, 3: n=14. The diagnostic accuracy of GRE images in assessing the iron content of tumor tissue accordingly was 88%, 79% and 81% with K values of 0.812, 0.683 and 0.715 for observer 1, 2, and 3 respectively. Interobserver agreement was excellent with kappa values ranging from 0.843 to 0.905. Overall, iron deposits were depicted on histopathology in 96.5% and on MR images in 93-96,5% of TGCTs. On GRE images the observers diagnosed involvement of joint compartments not seen on standard images alone in 6/58 (10%), 6/58 (10%), and 5/58 (8%) of cases.

Conclusions:

A T2*-weighted GRE sequence added to a standard MR protocol allows accurate and reproducible quantification of iron content in TGCTs. Due to the high incidence of iron deposits in these synovial lesions, this ability together with typical MR findings on T1 and T2 weighted images might be of help to

establish the diagnosis more confidently. Furthermore, GRE images depict tumor manifestations in joint compartments that can appear uninvolved on standard images and thus, are helpful in planning of surgical treatment.

Abbreviations:

TGCT: Tenosynovial giant cell tumor

PVNS: Pigmented villonodular synovitis

GRE: Gradient echo

MR: Magnetic Resonance

WHO: World Health Organisation

INTRODUCTION

Tenosynovial giant cell tumor (TGCT) has been classified as a neoplastic lesion from the group of the so called fibrohystiocytic tumours by the World Health Organization (WHO) in 2013 [1]. These benign lesions usually arise from the synovium of the joints, bursae and tendon sheath and can be subdivided according to their location, growth pattern and biologic behaviour into localized and diffuse types [1,2]. The localized type of TGCT occurs as a circumscribed tumor within tendon sheaths or joints, most often in the digits, knee, ankle and wrist [2,3]. The diffuse type of TGCT (former PVNS) shows a more aggressive growth pattern and predominantly affects the knee joint (73-80% of cases) followed in decreasing frequency by the hip, the ankle, the shoulder and the elbow joint [1,4-6].

Histologically, TGCT are characterized by the presence of a fibrous stroma with different proportions of mononuclear cells, multinucleate giant cells, macrophages and siderophages. Hemosiderin deposits in variable amounts represent another typical feature on pathologic examination [1,6].

MR imaging findings of intra- and extraarticular TGCT have been described in various articles and book chapters [3,7-22]. Some authors suggested the use of T2*-weighted gradient echo (GRE) sequences in order to depict susceptibility

artifacts (“blooming”) caused by the iron content of the tumor tissue and thus, to narrow the differential diagnosis [3,14-23]. However, little is known about the true frequency of this finding in the localized and diffuse type, and its value for defining the extent of the disease prior to surgery has not been determined in radiologic studies. Furthermore, it remains unclear whether a direct correlaton of MR findings and histologic quantification of hemosiderin deposition exists.

The purpose of our study was to evaluate the role of a T2*-weighted gradient echo (GRE) sequence added to a standard MR imaging protocol in assessing the iron content of tumor tissue and the extent of joint involvement in patients with tenosynovial giant cell tumor (TGCT).

MATERIALS AND METHODS

Study population

The study was approved by our institutional review board. The requirement for informed consent was waived. To identify patients, the radiologic data base of the musculoskeletal tumor center at our institution was searched from January 2002 to December 2013 using the key words “tenosynovial giant cell tumor “, “TGCT”, “giant cell tumor of the tendon sheath”, “pigmented villonodular synovitis”, “PVNS”, and “pigmented villonodular tenosynovitis”. The initial search identified a total of 301 patients. All diagnoses were cross-checked with

the pathology records of our institution. Inclusion criteria for the study population were as follows:

a) availability of a detailed pathology report from our institution with the final diagnosis of TGCT(PVNS),

b) MR examination performed at our institution with a standardized protocol which in addition to T1-, T2-weighted and CE SE/TSE sequences included a T2*-weighted GRE sequence,

c) surgical treatment either by arthroscopic synovectomy or open total synovectomy performed at our Institution.

Exclusion criteria were previous surgery (including prior biopsies) or radiation therapy, recurrent lesions, and incomplete MR examinations.

MR imaging

MR imaging was performed on 1.5 T systems (Magnetom Avanto, Siemens Medical Solutions, Erlagen Germany; Gyroscan NT Intera, Philips Medical systems, Best, The Netherlands) in 44 patients and on 3 T systems (Magnetom Verio, Siemens Medical Solutions; Ingenia, Philips Medical systems) in 14 patients. Depending on the site of the tumor, different dedicated surface coils and flexible coils were utilized. Contrast-enhanced images were obtained following the intravenous administration of a standard dose (0.1 mmol per

kilogram of body weight) of gadopentate dimeglumine (Magnevist; Bayer healthcare, Berlin Germany).

Parameters for all pulse sequences are presented in Table 1.

Image analysis

MR examinations were retrospectively and independently reviewed by three radiologists (K.W., S.W., D.M.) with 20, 15, and 3 years of experience in muskuloskeletal radiology, respectively. The three observers knew beforehand that all patient had pathologically confirmed TGCT (PVNS) but were unfamiliar with the cases. The image material was presented in random order and did not contain any patient information. Standard and GRE images were analyzed separately. At first, the three observers were asked to evaluate only the standard images. They had to describe the localisation (specific joint, tendon sheath, or bursa) and the manifestation type (localized or diffuse) of the disease. Whereas the localized type is characterized by a circumscribed (solitary) nodule with otherwise normal synovial structures, the diffuse type was diagnosed if more than one nodule and/or a more diffuse proliferation of synovial tissue was seen. The size of the lesions had to be determined by measuring the maximum diameter of the nodule (localized type) or by measuring the maximum length of the entire synovial mass (diffuse type). Measurements were performed with use of the integrated PACS measurement function. The predominant signal intensity

of the lesions was compared to that of muscle tissue on T1 weighted and to that of fat on T2 weighted MR images (without fat suppression) and graded as hypo-, iso- or hyperintense accordingly. The readers described the signal intensity of the tumor tissue on T1- and T2 weighted images as homogeneous, if all portions of the lesion had more or less the same signal intensity, and as inhomogeneous if the signal intensity varied among different portions of the lesion. The relative contrast enhancement of the tumor tissue was graded as absent, mild, moderate or marked and described as homogeneous, if the entire lesion showed the same amount of contrast enhancement, or as inhomogeneous if the grade of enhancement varied among different portions of the lesion.

Thereafter, the observers were asked to assess the extent and distribution of susceptibility artifacts on GRE images. The extent was graded as absent, focal, moderate/confluent or massive/diffuse. Focal susceptibility artifacts were small isolated areas of signal void within the tumor tissue. In contrast, moderate/confluent artifacts represented larger areas of signal void which could be confluent but did not extend over the entire mass. Massive/diffuse artifacts covered major portions of the tumor tissue with hardly any uninvolved areas.

Furthermore, the three observers analyzed the GRE images with a view to the identification of tumor tissue in joint compartments which appeared uninvolved on images of standard sequences (evidence of susceptibility artifact on GRE sequences with no obvious correlate on standard sequences). Intraoperative and histologic findings served as the standard reference.

Finally, the three observers evaluated the entire image sets for the presence of pressure erosions of bone, subchondral cysts, and bone marrow edema. A pressure erosion of bone was diagnosed if the bone immediately adjacent to the tumor or to a portion of the mass showed a well defined defect with a contour that followed the outer contour of the tumor. Subchondral cysts were defined as well-defined bone defects in the subchondral area which were either filled with fluid or with tumor tissue and thus, either exhibited signal intensities equivalent to those of water or to those of the extraossoeus component of the TGCT. Bone marrow edema was diagnosed, if the bone marrow adjacent to the tumor showed abnormal areas of high T2-weighted and decreased T1-weighted signal intensity. On T1-weighted images, the signal intensity had to be lower compared with normal fatty bone marrow and brighter compared with muscle tissue (in contrast to bone marrow replacement). The trabecular bone structure had to be preserved, and the margins to adjacent normal bone marrow were ill-defined.

Image quality was subjectively assessed by one observer by using a three point scale (excellent; good; poor).

Histopathologic Analysis

Fifty-eight cases of TGCT were included in the study. For histopathologic evaluation, specimen were fixed in 10% neutral buffered formalin, routinely processed and embedded in paraffin. 5 micron sections were stained with H&E

for routine evaluation and Prussian blue staining for evaluation of iron deposition. All slides were reviewed by a musculoskeletal pathologist (M.S.) with 6 years of experience in muskuloskeletal pathology. Diagnosis of TGCT (localized or diffuse type) was confirmed according to the WHO Classification of Tumors of Soft Tissue and Bone in all 58 patients. Iron deposition in the lesions was quantified in a four-tiered scale: grade 0 = no iron deposition, grade 1 = dot-like iron deposition (< 30% of tumor tissue), grade 2 = confluent iron deposition (30%-70% of tumor tissue), grade 3 = diffuse iron deposition (> 70% of tumor tissue). In cases of inhomogeneous staining, the grade, which was predominant in the tumor tissue was taken into the statistical evaluation.

Statistical Analysis

For categorical data absolute and relative frequencies are presented, quantitative measures are summarized by median, minimum, and maximum or mean and standard deviation. For assement of agreement between ratings and gold standard absolute and relative frequencies of concordance between rating and gold standard are presented with exact 95% confidence interval for the diagnostic accuracy. Additionally, weighted kappa values were estimated to evaluate each reader's agreement with the gold standard. Weighted kappa values are also presented for pairwise assessment of interrater agreement. Statistical analyses were performed with SAS version 9.3 and SPSS version 23.

RESULTS

Study Population

A total of 301 consecutive MR examinations were identified between January 2002 and December 2013. Of these 301 MR examinations, 243 were not included in the study group due to our inclusion and exclusion criteria. Recruitment of patients and the reasons for and numbers of exclusion are displayed in a flowchart in Fig. 1.

58 patients (23 male, 35 female) met the inclusion criteria and were included in the study. The patient mean age was of 36.7 years with a standard deviation of 13.9 years. The sites of involvement of the 58 patients included MR examinations of 44 knee joints, 5 hip joints, 5 ankle joints, 1 elbow joint, 1 flexor tendon sheath of the third finger, 1 intratarsal joint and 1 flexor hallucis longus tendon sheath.

The MR examinations of included patients were predominantly performed at 1.5 T (77.5%). Only 14 of 58 (22.5%) patients underwent MR investigation with the 3-T system.

The indications to undergo MR examination were either a slowly progressive pain with swelling (n=54) or decreased range of motion of the joint affected with joint effusion (n=37),

Image analysis

The lesions were localised in joints (n=56) or in tendon sheats (n=2). Bursae were additionally affected by the synovial profileration in the diffuse form of TGCT in 18 cases. Thirty-four (59%) lesions were classified as localized forms and twenty-four (41%) as diffuse TGCTs. The maximum diameter of the nodule (localized type) measured from 1.7 cm to 6.1 cm and the maximum length of the entire synovial mass (diffuse type) ranged from 2.7 cm to 14 cm.

On T1-weighted images the predominant signal intensity of the synovial proliferation was mainly classified as isointense and generally as homogenous. On T2-weighted images the three readers evaluated the synovial lesions as hypointense in all the patients 100%(58/58) and as inhomogeneous in the majority of lesions. The relative contrast enhancement of the tumor tissue was mainly graded as marked or moderate of our scale and described as inhomogeneous (Table 2).

Overall, iron deposits were seen on histopathology of TGCTs in 56/58 (96.5%) patients and on MR images in 56/58 (96.5%), 55/58 (94.8%) and 54/58 (93.1%) for observer 1, 2, and 3 respectively. The signal void caused by hemosiderin deposition in the tumorous mass was assessed as a grade 3 in 13/58 (22.4%), 14/58 (24.1%) and 15/58 (25.8%) patients, as a grade 2 in 29/58 (50%), 25/58 (43.1%), and 25/58 (43.1%) patients, as a grade 1 in 14/58 (24.1%), 16/58

(27.5%) and 14/58 (24.1%) patients and no signal void was described in 2/58 (3,4%), 3/58 (5,1%) and 4/58 (6.8%) cases. The histological evaluation quantified the iron deposition of the tissue specimen as a grade 3 in 14/58 (24.1%), a grade 2 in 29/58 (50%), a grade 1 in 13/58 (22.4%) and showed no evidence of iron deposition in 2/58 (3.4%) cases (Figs 2 - 4).

The observers main tendency was to underrate rather than overrate the iron quantification with percentage values ranging from 6.9% (4 patients) to 13.8% (8 patients). Considering the histological evaluation of the iron content of the lesions as the reference standard the diagnostic accuracy of T2*-weighted GRE images in assessing the iron content of tumor tissue was 88% (95% confidence interval: 77% to 95%), 79%, (67% to 89%) and 81% (69% to 90%). The weighted Kappa value for the correlation of the radiological and the histopathological grading was consistent with values of 0.812, 0.683 and 0.715 for observer 1, 2 and 3 respectively. The Interobserver agreement of the radiological evaluation of the extent and distribution of the blooming artifact was substantial with weighted kappa values ranging from 0.843 to 0.905 (Table 3).

On GRE images the three observers diagnosed involvement of joint compartments not seen on standard images alone in 6/58 (10.3%), 6/58 (10.3%), and 5/58 (8.6%) of cases, respectively (Fig 5). The observers agreed in four patient and described tumor tissue in the posterior region of the knee joint in two patients, posterior to the medial meniscus in one patient and in the dorsal aspect

of the tibiotalar joint, regions which appeared uninvolved on standard images. The findings assessed on T2* GRE images changed the radiological diagnosis from that of a focal to a diffuse TGCT in six (10.3%), five (8.6%) and four (6.8%) cases for observer 1, 2 and 3 respectively. Intraoperative and histologic findings served to verify the locations assessed by the radiologist. The depiction of tumor tissue in joint compartments which appeared uninvolved on standard images was considered helpful in planning of surgical treatment changing the synovectomy approach.

Evaluating the entire set of images evidence of pressure bone erosions was described in 23/58(39.6%), 22/58(37.9%) and 21/58(36.2%) patients, of subchondral cyst 8/58(13.7%), 12/58(20.6%) and 8/58(13.7%) patients and bone marrow edema in 1/58(1.7%), 4/58(6.8%) and 2/58(3.4%) patients (Fig. 6).

Image quality was assessed as excellent in 33(56.8%) and good in 25(43.1%) examinations by observer 1.

Histopathology

In all fifty-eight cases surgical tumor resection was performed at our Institution between 2002 and 2013. Histopathologic analysis of resected specimen showed TGCT according to the criteria of the WHO classification of Tumors of Soft Tissue and Bone in all cases [1].

According to the four-tiered scale, iron deposition was quantified. Iron was detected either in macrophages or diffuse within tumor stroma. We found iron staining in > 70% of tumor tissue (grade 3) in 14/58 (24.1%) cases, confluent iron staining in 30-70% of tumor tissue (grade 2) in 30/58 (51.7%) cases and dot-like iron staining in < 30% of tumor tissue (grade 1) in 12/58 (20.7%) of cases. No iron staining was found in 2/58 (3.4%) cases. (Figs 2 - 4 HE, grade 2, 3, 4)

Discussion

In the present study we have demonstrated that in patients with TGCT the blooming artifact sign depicted on T2* GRE sequence is accurate in the evaluation of hemoglobin iron content with histopathological analysis as a reference standard. Another important result of our study was that a T2* GRE sequence added to a standard MR protocol is useful in assessing the extent of joint involvement in patients with TGCT.

A total of 58 patients with histologically proven TGCT were evaluated. Most of the lesions were located in the knee joint (72.4%) clearly outnumbering those in other localisations [4,5]. Furthermore, the mean age of the patients (36.7) and the sex distribution with a prevalence of female patients (60%) are similar to those of previous studies [4,5,22]. Therefore, our study population is comparable to other study populations and can be regarded as representative.

In accordance with other studies, the tumors included in our series typically showed homogeneous intermediate to low SI compared to muscle on T1 weighted images [3,7-22]. In few patients MR examinations depicted areas of high signal intensity that, as described by other authors, might represent lipid-laden areas [15-18,24]. Due to the shortening of T2 relaxation time caused by hemosiderin intermediate to low signal intensity also predominates on T2-weighted MR images [3,7-22]. This effect is accentuated at higher field strength [15,17,18]. In our series all lesions were assessed as hypointense compared to fat on T2-weighted images. Contrast-enhancement is a typical but variable feature of TGCT [3,8,15-22]. Almost all lesions in our series showed a marked or moderate degree of enhancement and its pattern was mainly diagnosed as inhomogenous.

On MR examinations, GRE sequences are sensitive to magnetic field inhomogeneity caused by magnetic susceptibility differences between tissues. Magnetic field inhomogeneities generally occur at the interface among tissues with different magnetic susceptibilities and causes the susceptibility artifact reported in terms of T2* signal decay [23]. On gradient-echo images in patients affected by TGCT the signal void is particularly evident with an enlargement of the low-signal-intensity areas ("blooming artifact") caused by the magnetic susceptibility artifact [17,18,21,22]. Hemosiderin a breakdown product of hemoglobin in variable amounts represents a typical feature of TGCT on pathologic examination [6]. Multinucleate giant cells derived from macrophages

and synovial lining cells may also contain hemosiderin [6]. Evidence of blooming artifact was assessed in almost all the patients in this study. The three readers reported no signal void on T2* GRE images of two localised TGTTs. Correspondingly, histological analysis showed no evidence of iron staining in these lesions. The histological report assessed evidence of iron deposits in 96.5% (56/58) of the patients. Due to the high incidence of iron deposits of these synovial lesions, evidence of iron deposits on T2* GRE images together with classical MR findings on T1 and T2 weighted images might be of help to establish the diagnosis of TGCT more confidently. Therefore a T2* GRE should be added to a standard tumor imaging protocol if a synovial tumor (intraarticular or tenosynovial) is seen on standard images.

In our study the agreement between observers and histopathologic analysis in assessing the quantification of iron content of the tumor lesion was consistent. The observers tended to underestimate rather than overestimate the evaluation of the hemosiderin content of the synovial proliferation.

Treatment of TGCT is required to avoid destruction and progressive loss of function of the joint involved (in diffuse intraarticular form) or the tendon or bursa (in localized extraarticular disease) [26]. Surgical excision is the preferred treatment for all forms of TGCT [18,26,30]. The localised form of TGCT of the knee is treated arthroscopically through standard portals (anteromedial, anterolateral, and superomedial) while the diffuse form of TGCT requires specialised arthroscopic portals (posteromedial and posterolateral) or an open

surgical resection [28-30]. Regardless the surgical approach, complete resection of tumor tissue is required to reduce the likelihood of recurrence [18,27,28,30]. In the present study all patients underwent surgical resection either by arthroscopic or open surgical procedures. The depiction of additional areas of involvement on T2* GRE images changed the radiological diagnosis from that of a focal to a diffuse form of TGCT in only a small number of patients but was helpful for planning of surgical treatment in these cases. To our knowledge, few studies evaluated the tumor extent and the involvement of the joint by MR Imaging [20-22]. Kitagawa and coworkers [20] assessed the accuracy of MR imaging in the evaluation of the tumor size and the degree of extent around the phalanx which can effect the planning of the surgical procedure. Eckhardt *et al.* [21] assessed in pediatric patients a better estimate of the disease's extent in gradient-echo imaging. Cheng *et al.* [22] demonstrated in 23 patients that MR imaging is valuable in depicting the extent of the lesions.

In TGCT bone changes begin with bone erosion, often near the chondroosseous junction, with subsequent extension of the process and formation of juxtaarticular cysts surrounded by fibrous tissue [6]. Pressure erosions of bone occur more frequently in the hip and shoulder [15] than in the knee joint [6,15,16]. We assessed bone erosions in 25% of the patients with a substantial agreement between readers. Bone erosions of the knee joint were described in at least the 30% of the patients by the observers. The frequency of osseous erosions in our study population was higher compared to prior studies

[4,5,22,25]. Cheng and coworkers [22] assessed evidence of bone marrow edema in 10 of the 23 patients analyzed. In our series bone marrow edema was reported in a few patients with no specific localisation. Hughes and coworkers [17] reported bone erosion or subchondral cyst (62% of cases), edema in the adjacent bone (23 % of cases) as additional MR imaging findings of diffuse intraarticular PVNS. Compared to Hughes et al. [17] in our study subchondral cysts were reported mainly in knee affected by TGCT in a lower percentage.

Several limitations of our study should be considered. This study was limited by its retrospective nature and bias in that the three reviewers of the MR images knew beforehand that all patients had pathologically confirmed TGCT. No other synovial lesions were included in the study. This factor may have increased the sensitivity of detection of each MR findings. The three readers had different levels of experience. No one to one comparison histology/MR was performed. Finally, the sample study in our study is relatively small.

In summary, a T2*-weighted GRE sequence added to a standard MR protocol allows accurate and reproducible quantification of iron content in TGCTs. Due to the high incidence of iron deposits in these synovial lesions, this ability together with typical MR findings on T1 and T2 weighted images might be of help to establish the diagnosis more confidently. GRE images depict tumor manifestations in joint compartments that can appear uninvolved on standard images and thus may be helpful in planning the surgical treatment.

Table 1.
Parameters of MRI sequences.

Sequence and Field Strenght	Repetition Time (msec)	Echo Time (msec)	Flip Angle	FOV	Section Thickness	In-Plane Resolution
Coronal or sagittal T1W TSE* pre/post Gd						
1.5 T	413 - 929	14 – 28,8	90	160 - 180	3	< 0.5 x 0.5
3.0 T	511 - 989	12 – 21,2	180	160 - 200	3	< 0.5 x 0.5
Axial or sagittal T2W TSE						
1.5 T	3750 - 8620	83 - 113	180	160 - 180	3 - 5	< 0.5 x 0.5
3.0 T	2688 - 7529	85 - 120	159	160 - 200	3 - 5	< 0.5 x 0.5
Axial fat-saturated T1W TSE post Gd						
1.5 T	513 - 886	10 - 20	90	160 - 180	3 - 5	< 0.5 x 0.5
3.0 T	519 - 1020	13 – 21,2	180	160 - 200	3 - 5	< 0.5 x 0.5

Coronal or sagittal T2* GRE						
1.5 T	413 - 929	14 – 28,8	25	160 - 180	3	< 0.7 x 0.6
3.0 T	386 - 783	9,21 – 19,9	20	160 - 200	3	< 0.8 x 0.8

Note. T1W = T1 weighted, T2W = T2 weighted, TSE = turbo spin echo, GRE = gradient echo, Gd = intravenous gadolinium application

Table 2. MR characteristics of the TGCT.

T1 weighted signal	**Reader 1**	**Reader 2**	**Reader 3**
Hyperintense	1.7% (1/57)	1.7% (1/57)	5.2% (3/57)
Isointense	87.7% (50/57)	82.4% (47/57)	84.2% (48/57)
Hypointense	10.5% (6/57)	15.7% (9/57)	10.5% (6/57)
Homogeneous	78.9% (45/57)	63.1% (36/57)	61.4% (35/57)
Inhomogeneous	21% (12/57)	36.8% (21/57)	38.5% (22/57)
T2 weighted signal	**Reader 1**	**Reader 2**	**Reader 3**
Hyperintense	0% (0/58)	0% (0/58)	0% (0/58)
Isointense	0% (0/58)	0% (0/58)	0% (0/58)
Hypointense	100% (58/58)	100% (58/58)	100% (58/58)
Homogenous	43.1% (25/58)	39.6% (23/58)	37.9% (22/58)
Inhomogenous	56.8% (33/58)	60.3% (35/58)	62.1% (36/58)
Contrast enhancement	**Reader 1**	**Reader 2**	**Reader 3**
Marked	27.5% (16/57)	57.8% (33/57)	56.1% (32/57)
Moderate	59.6% (34/57)	24.5% (14/57)	29.8% (17/57)
Mild	12.2% (7/57)	15.7% (9/57)	12.2% (7/57)
No evidence	0% (0/57)	1.7% (1/57)	1.7% (1/57)
Homogenous	40.3% (23/57)	24.5% (14/57)	12.2% (7/57)
Inhomogenous	59.6% (34/57)	75.4% (43/57)	87.7% (50/57)

Table 3.
Results.

	Reader 1	**Reader 2**	**Reader 3**
Agreement Reader - Pathologist	51/58	46/58	47/58
Overrated	5.1% (3/58)	6.9% (4/58)	6.9% (4/58)
Underrated	6.9% (4/58)	13.8% (8/58)	12% (7/58)
Diagnostic Accuracy	88%	79%	81%
95% CIs	77% - 95%	67% - 89%	69% - 90%
K value	0.812	0.683	0.715
Interobserver κ value overall	With Reader 2: 0.857 With Reader 3: 0.843	With Reader 1: 0.857 With Reader 3: 0.905	With Reader 1: 0.843 With Reader 2: 0.905

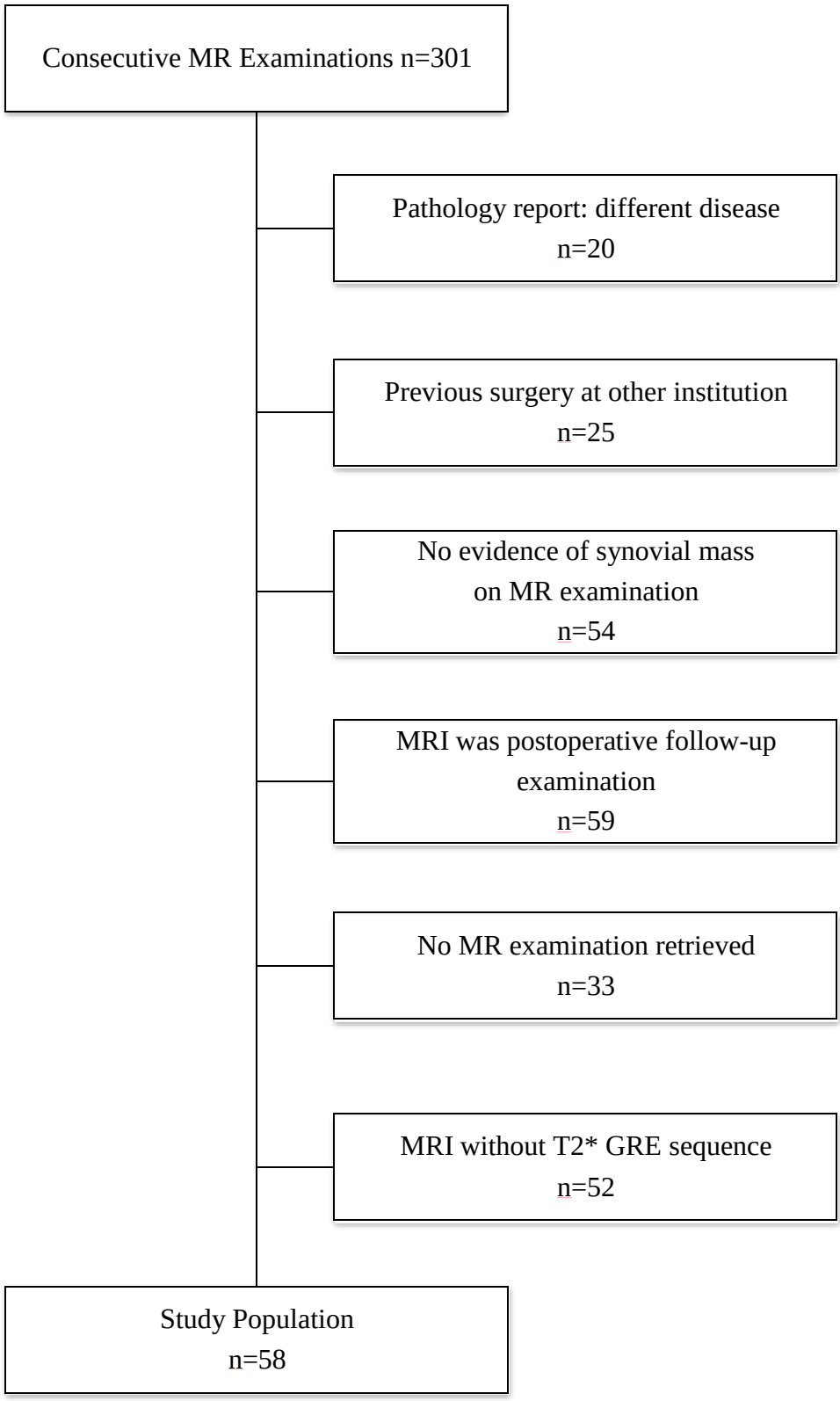

Figure 1: Flowchart of study population and patient recruitment.

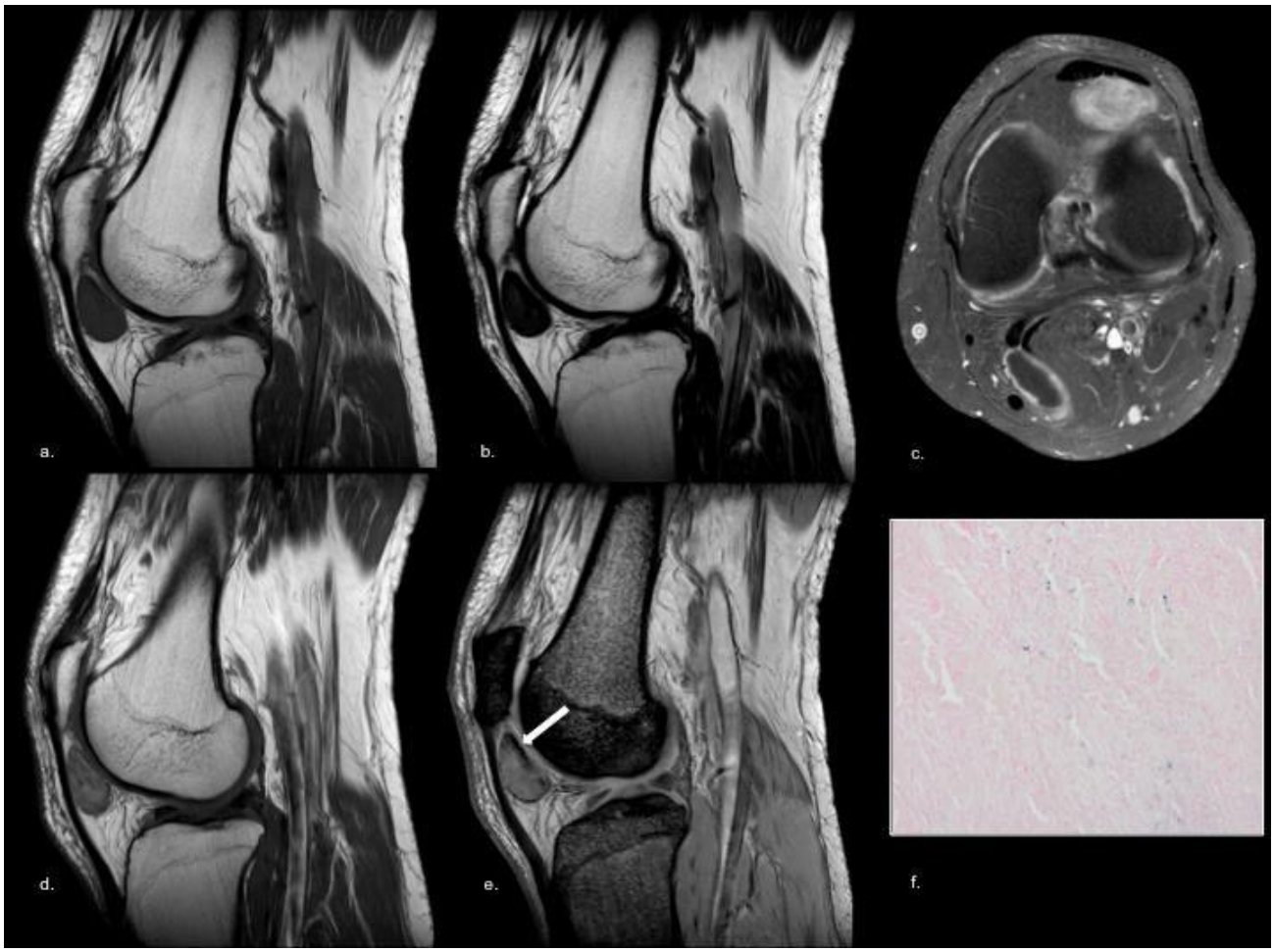

Fig 2. Focal form of TGCT of the knee.

a. sagittal T1 weighted TSE, b. sagittal T2 weighted TSE, c. axial T1 weighted with fat suppression after intravenous administration of gadolinium, d. sagittal T1 weighted after intravenous administration of gadolinium, e. sagittal T2* weighted GRE, d. 5 micron section stained with H&E for routine evaluation and Prussian blue staining for evaluation of iron deposition.

The MR examination shows a rounded mass located in Hoffa's fat pad of the left knee in a 60 year old male patient. The mass shows low signal intensity on T1 and T2 weighted images and a peripheral signal reduction in the posterior part of the lesion

(white arrow) on T2* wieghted GRE image. The tumor histology panel shows marginal iron deposition. The observers quantified the amount of blooming artifact as grade 1 which corresponded to the quantification of iron deposition assessed on pathology.

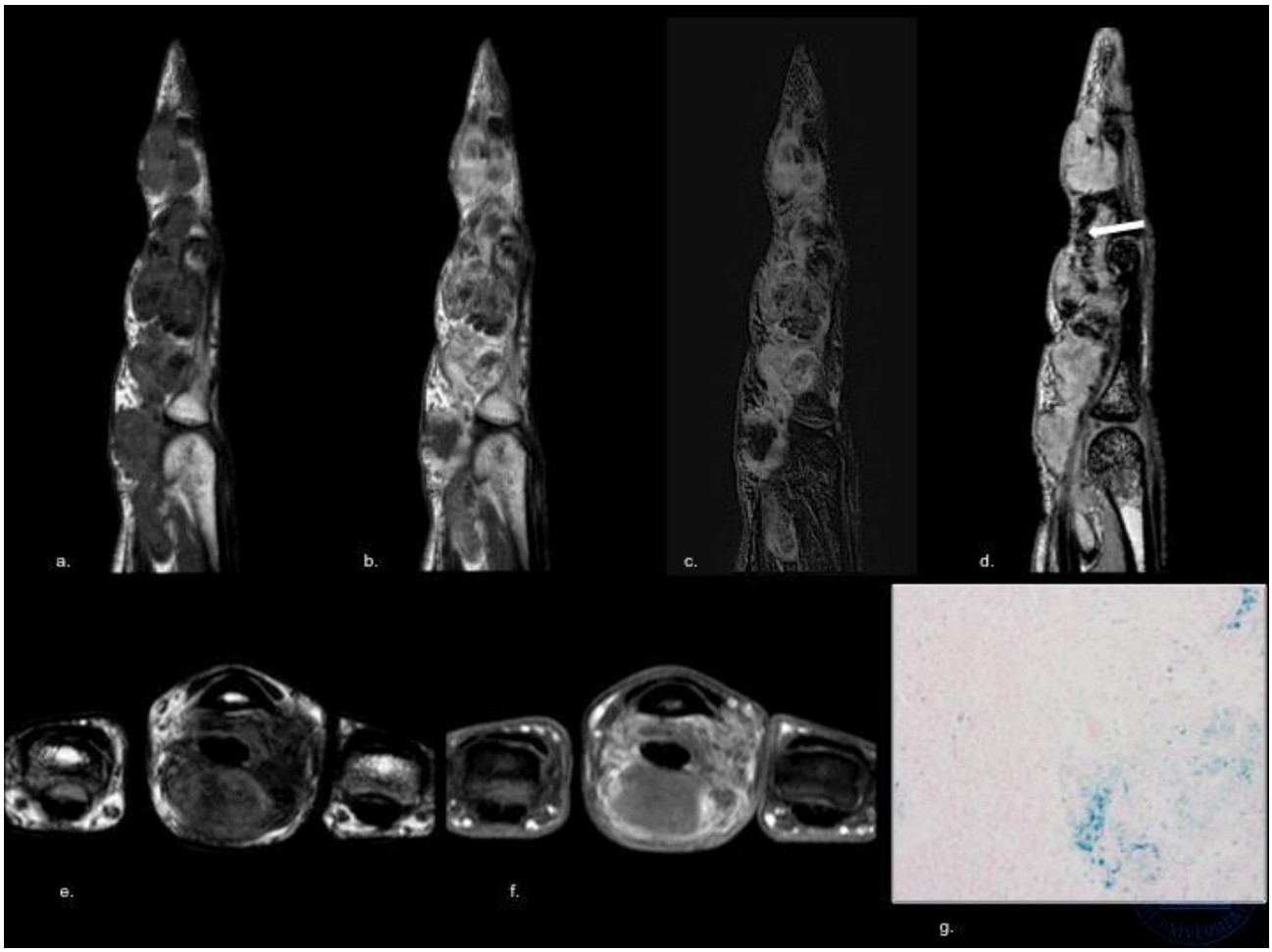

Fig 3. Diffuse form of TGCT of the finger.

a. sagittal T1 weighted TSE, b. sagittal T1 weighted TSE after intravenous administration of gadolinium, c. sagittal T1 weighted TSE subtraction sense after intravenous administration of gadolinium, d. sagittal T2* weighted GRE, e. axial T2 weighted TSE, f. axial T1 weighted SPIR after intravenous administration of gadolinium, g. 5 micron section stained with H&E for routine evaluation and Prussian blue staining for evaluation of iron deposition.

The MR examination shows a mass within the flexor tendon sheath of the third finger in a 53 year old female patient.. Low signal intensity predominates on T1 and T2

weighted images. The T2* weighted GRE sequence shows signal reduction in the posterior part of the lesion (white arrow). After contrast administration the lesion shows peripheral enhancement. Histology revealed confluent iron deposition. The observers described the amount of the blooming artifact as a grade 2 (moderate/confluent) which corresponded to the pathologist’s evaluation.

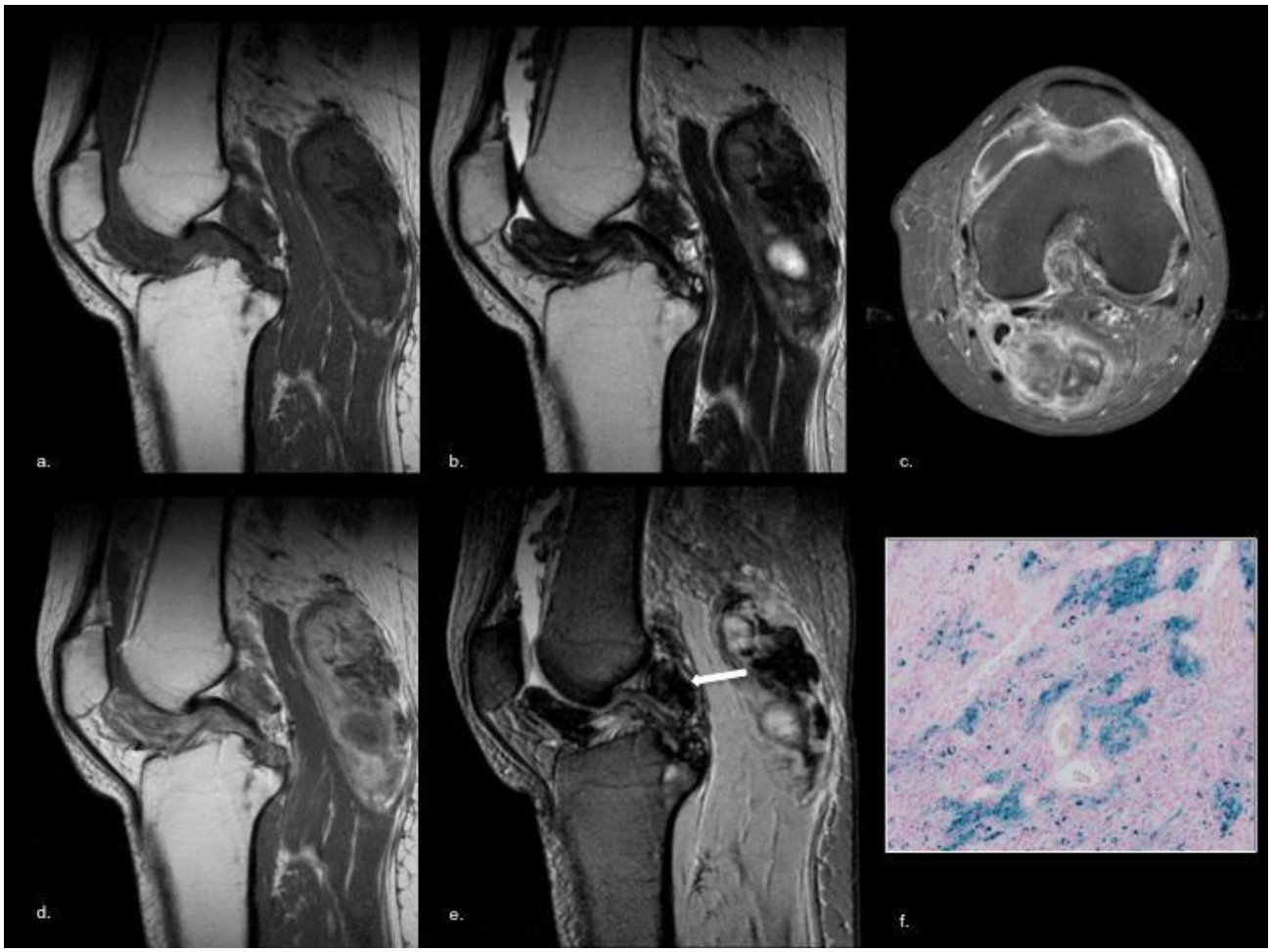

Fig 4. Diffuse form of TGCT of the knee.

a. sagittal T1 weighted TSE, b. sagittal T2 weighted TSE, c. axial T1 weighted with fat suppression after intravenous administration of gadolinium, d. sagittal T1 weighted after intravenous administration of gadolinium, e. sagittal T2* weighted GRE, d. 5 micron section stained with H&E for routine evaluation and Prussian blue staining for evaluation of iron deposition.

MR images show a diffuse mass affecting the entire knee joint of a 23 year old female patient. The largest portion of the tumor is located in the bursa of the semimembranous muscle. Histology showed diffuse iron deposition. The observers

described the amount of blooming artifact (white arrow) as a grade III (massive/diffuse) which corresponded to the pathologist's assessment.

Fig 5. Additional localisations of TGCT on T2* GRE.

a. axial T1 weighted with fat suppression, b. sagittal T2 weighted TSE, c. sagittal T1 weighted with fat suppression after intravenous administration of gadolinium, d. sagittal T2* weighted GRE.

The MR examination shows a mass in the anterior joint recess of the ankle in a 40 year old female patient. The lesion demonstrates low signal intensity on T1 and T2 weighted images. Note bony erosion at the anterior tibia and talus. The T2* GRE weighted image clearly shows an additional nodular manifestation in the posterior

joint recess (white arrow), which was not diagnosed on images of the standard sequences.

Fig 6. Additional findings.

a. sagittal T1 weighted TSE, b. sagittal T2 weighted TSE, c. sagittal T2* weighted GRE, d. sagittal T1 weighted TSE, e. sagittal T1 weighted TSE with fat suppression after intravenous administration of gadolinium, f. sagittal T2* weighted GRE.

Additional findings in patients affected by TGCT are bone erosions at the bare areas, subchondral cysts and bone marrow edema. (a-c) The images of the right knee show large cystic lesions in the lateral tibial plateau (white arrow) in a 36 year old male patient with dffuse type TGCT. (d-f) In the left ankle of a 48 year old female patient with diffuse type TGCT in the anterior joint recess pressure erosion at the talar neck

and the anterior tibia (black arrows) as well as bone marrow edema of the talus (arrowhead) are seen.

References

1. C.D.M. Fletcher, J.A. Bridge, P.C.W. Hogendoorn, F. Mertens, WHO Classification of Tumours of Soft Tissue and Bone, Volume 5, fourth ed, 2013, pp. 99-103.
2. H. Jaffe, L. Lichtenstein, C. Sutro, Pigmented villonodular synovitis, bursitis and tenosynovitis: a discussion of the synovial and bursal equivalents of the tenosynovial lesion commonly denoted as xanthoma, xanthogranuloma, giant cell tumor or myeloplaxoma of tendon sheath with some consideration of this tendon sheath lesion itself, Arch Pathol. 31 (1941) 731-765.
3. D.W. Stoller, P.F.J. Tirman, M.A. Bredella, S. Beltran, R.M. Branstetter III, S.C.P. Blease, Ed Amirsys, Diagnostic Imaging Orthopaedics, first ed. second printing June 2004. pp. 90-93,140-143.
4. S. Ottaviani, X. Ayral, M. Dougados, L. Gossec, Pigmented villonodular synovitis: a retrospective single-center study of 122 cases and review of the literature, Semin Arthritis Rheum. Jun 40(6) (2011) 539-46.
5. G.P. Xie, N. Jiang, C.X. Liang, J.C. Zeng, C.Y. Chen, Q. Xu, R.Z. Qi, Y.R. Chen, B. Yu, Pigmented villonodular Synovitis: a retrospective multicenter study of 237 cases, Plos One. Mar 23,10(3) (2015) e0121451.
6. R.H. Dorwart, H.K. Genant, W.H. Johnston, J.M. Morris, Pigmented villonodular synovitis of synovial joints: clinical, pathologic, and radiologic features, AJR Am J Roentgenol. 143 (1984) 877-885.

7. S. Khan, C.H. Neumann, L.S. Steinbach, K.D. Harrington, MRI of giant cell tumor of the tendon sheath of the hand: a report of three cases, Eur Radiol. 5 (1995) 467-470.
8. L. De Beuckeleer, A. De Schepper, F. De Belder, J. Van Goethem, M.C. Marques, J. Broeckx et al. Magnetic resonance imaging of localized giant cell tumor of the tendon sheath (MRI of localized GCTTS), Eur Radiol. 7 (1997) 198-201.
9. J.S. Jelinek, M.J. Kransdorf, J.A. Utz, B.H. Berrey jr, J.D. Thomson, R.D. Heekin, et al, Imaging of pigmented villonodular synovitis with emphasis on MR imaging, AJR Am J Roentgenol. Feb152(2) (1989) 337-42.
10. D. Karasick, S. Karasick, Giant cell tumor of tendon sheath: spectrum of radiologic findings, Skeletal Radiol. 21(4) (1992) 219-24.
11. S.J. Lynskey, M.J. Pianta, MRI and thallium features of pigmented villonodular synovitis and giant cell tumours of tendon sheaths: a retrospective single centre study of imaging and literature review, BR J Radiol. Dec88 (2015) (1056):20150528.
12. K.W. Kim, M.H. Han, S.W. Park, S.H. Kim, H.J. Lee, H.J. Jae, et al, Pigmented villonodular synovitis of the temporomandibular joint: MR findings in four cases, Eur J Radiol. Mar49(3) (2004) 229-34.
13. J.K. Jelinek, M.J. Kransdorf, B.M. Shmookler, A.A. Aboulafia, M.M. Malawer, Giant cell tumor of the tendon sheath: MR findings in nine cases, AJR Am J Roentgenol. Apr162(4) (1994) 919-22.

14.J. Llauger, J. Palmer, J.M. Monill, T. Franquet, S. Baqué, N. Rosón, MR imaging of benign soft-tissue masses of the foot and ankle, Radiographics. Nov-Dec18(6) (1998) 1481-98.

15.J. Llauger, J. Palmer, N. Rosón, R. Cremades, S. Bagué, Pigmented villonodular synovitis and giant cell tumors of the tendon sheath: radiologic and pathologic features, AJR Am J Roentgenol. 172 (1992) 1087-1091.

16.J. Lin, J.A. Jacobson, D.A. Jamadar, J.H. Ellis, Pigmented villonodular synovitis and related lesions: the spectrum of imaging findings, AJR Am J Roentgenol. 172 (1999) 191-197.

17.T.H. Hughes, D.J. Sartoris, M.E. Schweitzer, D.L. Resnick, Pigmented villonodular synovitis: MRI characteristics, Skeletal Radiol. 24 (1995) 7-12.

18. M.D. Murphey, J.H. Rhee, R.B. Lewis, J.C. Fanburg-Smith, D.J. Flemming, E.A. Walker, Pigmented villonodular synovitis: radiologic-pathologic correlation, Radiographics. 28(5) (2008) 1493-518.

19.H.W. Garner, C.J. Ortiguera, R.E. Nakhleh, Pigmented Villonodular Synovitis, Radiographics. 28 (2008) 1519–1523.

20.Y. Kitagawa, H. Ito, Y. Amano, T. Sawaizumi, T. Takeuchi, MR imaging for preoperative diagnosis and assessment of local tumor extent on localized giant cell tumor of tendon sheath, Skeletal Radiology. Nov;32(11) (2003) 633-8.

21.B.P. Eckhardt, R.J. Hernandez, Pigmented villonodular synovitis: MR imaging in pediatric patients, Pediatric Radiology. 34 (2004) 943-947.

22. X.G. Cheng, Y.H. You, W. Liu, T. Zhao, H. QU, MRI features of pigmented villonodular synovitis (PVNS), Clin Rheumatol. Feb;23(1) (2004) 31-4.

23. R. Bitar, G. Leung, R. Perng, S. Tadros, A.R. Moody, J. Sarrazin J, et al, MR pulse sequences: what every radiologist wants to know but is afraid to ask, RadioGraphics. 26 (2006) 513–537.

24. M.J. Kransdorf, M.D. Murphey, Synovial tumors, In: Imaging of soft tissue tumors, Pa: Lippincott Williams & Wilkins, Philadelphia, 2006; 381–436.

25. H.D. Dorfman, B. Czerniak, Synovial lesions, In: Bone tumors. Mo: Mosby, St Louis, 1998; 1061-1071.

26. K.R. Chin, S.J. Barr, C. Winalski, D. Zurakowski, G.W. Brick, Treatment of advanced primary and recurrent diffuse pigmented villonodular synovitis of the knee, J Bone Joint Surg Am. 84 (2002) 2192–2202.

27. E. Palmerini, E.L. Staals, R.G. Maki, S. Pengo, A. Cioffi, M. Gambarotti, et al, Tenosynovial giant cell tumour/pigmented villonodular synovitis: outcome of 294 patients before the era of kinase inhibitors, Eur J Cancer. Jan;51(2) (2015) 210-7.

28. H. Sharma, B. Rana, A. Mahendra, M.J. Jane, R. Reid, Outcome of 17 pigmented villonodular synovitis (PVNS) of the knee at 6 years mean follow-up, Knee. Oct;14(5) (2007) 390-4.

29. D.J. Ogilvie-Harris, J. Mc Lean, M.E. Zarnett, Pigmented villonodular synovitis of the knee. The results of total arthroscopic synovectomy, partial,

arthroscopic synovectomy, and arthroscopic local excision, J Bone Joint Surg Am. Jan;74(1) (1992) 119-23.

30. J.C. Aurégan, S. Klouche, Y. Bohu, N. Lefèvre, S. Herman, P. Hardy, Treatment of pigmented villonodular synovitis of the knee, Arthroscopy. Oct;30(10) (2014) 1327-41.